Int. J. Solids Structures Vol. 26, No. 5/6, pp. 511–525, 1990
Printed in Great Britain.

0020-7683/90 $3.00 + .00

A GEOMETRICALLY NONLINEAR MODEL FOR PREDICTING THE INTRINSIC FILM STRESS BY THE BENDING-PLATE METHOD

BRIAN D. HARPER
Department of Engineering Mechanics, The Ohio State University, Columbus, OH 43210-1181, U.S.A.

and

CHIH-PING WU
Department of Civil Engineering, National Cheng Keng University, Tainan, Taiwan, R.O.C.

(*Received* 14 *September* 1988; *in revised form* 7 *April* 1989)

Abstract—This study presents a new method for calculating the intrinsic stress that develops in a film as it is deposited onto a substrate. Previous investigations have employed a simplified, geometrically linear beam or plate theory that assumes very thin films and, in most cases, a uniform film stress in order to calculate the film stress from measured deflections of the substrate. The model presented here makes no assumptions regarding the thickness of the film or the uniformity of the film stress and also accounts for nonlinear geometric effects which may become singificant whenever the measured deflections reach an order of magnitude equal to or greater than that of the substrate thickness. Results are presented based upon material properties and geometrical parameters that are typical for the bending-plate experiment. Comparisons are also made based upon actual experimental data that have appeared in the literature. These results clearly indicate the significance of nonlinear geometric effects in the bending-plate experiment. The model developed here may be used either to directly account for these effects or to design an experiment in such a way that these effects will be negligible.

INTRODUCTION

Intense stresses are known to develop in thin films as they are deposited onto a substrate material. Since these stresses are often comparable to the thin film materials bulk yield stress, it is anticipated that they could have significant effects upon the material's mechanical, electrical, magnetic and optical properties. For this reason, thin film stresses have been studied extensively for many years and a large body of literature has subsequently developed. It is beyond the scope of the present paper to present a detailed review of this literature. Interested readers are referred to three excellent review articles by Hoffman (1966), Chopra (1969) and Kinosita (1972).

Several mechanisms accounting for the development of thin film stresses have been proposed in the literature and are reviewed by Chopra (1969). From a macro-mechanics point of view the detailed mechanism is unimportant, and it is sufficient to assume that during its deposition, the film undergoes some type of microstructural change which induces a non-mechanical or "intrinsic" strain. Stresses develop since this intrinsic strain acts against a geometrical constraint imposed by the adjacent substrate material. Since this intrinsic strain is a non-mechanical strain (i.e. a strain that does not produce stress in the absence of geometrical constraints), it may be considered analogous in its effects to a thermal strain.

Of the various experimental methods that have been employed to indirectly estimate the stresses in thin films, it is the so-called bending-plate or bending-beam method which has received the widest application. In this experiment, a thin film (up to around 2000 Å) is deposited onto a relatively thin (≈ 0.1 mm) usually rectangular substrate. The intrinsic strain that develops in the film produces an effective eccentric loading on the substrate which, if the substrate is thin enough, will result in measurable out-of-plane displacements. These displacements are used to calculate the specimen's curvature and a simple theory is applied to determine the film stress. Needless to say, the stress calculated in this manner cannot be more accurate than the assumptions that are employed in the development of

this "simple" theory. The purpose of the present paper is to investigate the appropriateness of a few of these assumptions emphasizing, in particular, the key assumption of linear strain/displacement relations (i.e. the assumption that the displacements are small with respect to substrate thickness). This assumption is considered to be critical from a practical point of view since it represents a fundamental dilemma for the experimentalist. On the one hand, he would like to use as thin a substrate as possible so that the out-of-plane deflections may be easily and precisely measured, while on the other hand he must always guarantee that the deflections measured are at least an order of magnitude less than the substrate thickness if a linear theory is to be employed to calculate the film stress. Thus, any decrease in thickness of the substrate employed results in a decrease in the acceptable range of deflections that may be measured.

Unfortunately, most of the published experimental results fail to report the dimensions of the substrate that was employed so that it is rather difficult to make a general assessment of the relative magnitude of the measured deflections with respect to substrate thickness. Chopra (1969), however, does state that "the measured displacements often are not much smaller than the substrate thickness". If this does indeed turn out to be the rule rather than the exception, then the use of a linear theory to predict film stresses must be considered questionable, and many of the published results may be misleading. Chopra (1969) addressed this question by making an analogy with a known large deflection solution for an isotropic plate loaded by pure bending moments applied only to two opposite edges. From this he concluded that significant discrepancies between the linear and nonlinear results would not occur even when the deflections are of the same order of magnitude as the thickness. This argument, however, is not convincing since the intrinsic film strain produces an effective eccentric loading on the substrate which is statically equivalent to an in-plane force as well as a bending moment. The presence of an in-plane force is significant since an appreciable amount of the nonlinearity in these problems may be attributed to the coupling between in-plane forces and out-of-plane deflections in the plate equilibrium equations. One of the objectives of the present paper is to address this problem by developing a nonlinear model that is directly applicable to the bending-plate experiment that is used to measure film stresses.

PROBLEM FORMULATION

Most applications of the bending-plate experiment involve the deposition of a thin film onto a rectangular, usually beam-like substrate. According to Chopra (1969), this beam-like substrate is either rigidly clamped at one end (cantilevered beam) or is supported on knife edges at both ends (simply supported beam). The most commonly employed models of the bending-plate experiment (see, for example, Stoney, 1909 and Brenner and Senderoff, 1949) were derived by assuming that the film/substrate laminate is free of external constraints. This situation corresponds directly to a beam with simple supports. Since these models are geometrically linear, they may also be considered applicable to the cantilevered beam provided, of course, that the curvature is calculated from relative displacements that are measured at locations far removed (in comparison to the beam width) from the clamped end.

Whenever nonlinear geometric effects are present, the specific support conditions may have a significant effect upon the resulting shape of the film/substrate laminate. For example, the nonlinear results developed later in this paper contain a critical or bifurcation point beyond which multiple solutions (shapes) are predicted. It is possible that one of these shapes may be inhibited by a clamped boundary. It is also conceivable that an entirely different shape might result due to a clamped boundary than would occur with simple supports. In the present work, the film/substrate laminate is assumed to be free of external constraints so that all nonlinear results should be considered strictly applicable only to cases involving a simply supported substrate.

Consider now a rectangular plate (Fig. 1) of length $2a$, width $2b$, and thickness h that has been fabricated by depositing a film layer of thickness h_f onto a substrate layer of thickness h_s and assume that the film and substrate are perfectly bonded, i.e. assume that

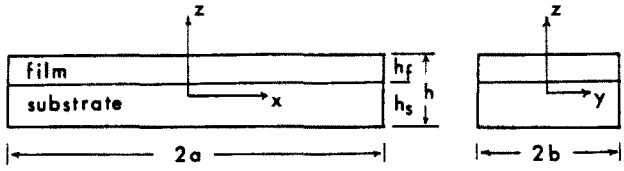

Fig. 1. Schematic of a rectangular film/substrate laminate.

the displacement field is continuous across the interface. Also assume that both the film and substrate are linear elastic and isotropic and that the in-plane dimensions of the plate are very large with respect to its thickness. Previous investigators have also assumed that the film is "very thin" in comparison with the substrate and, in some instances, that the film stress is distributed uniformly across the film thickness. The present development will not include any assumptions with regard to either the film thickness or the uniformity of the film stress.

In our opinion, the easiest and most direct approach to this problem is to consider the film and substrate layers to act as a single unit or "laminate" and then to employ the assumptions of classical lamination theory (see Jones, 1975) to write the stresses in the film and substrate layers in terms of the strains and curvatures of the middle-plane of the laminate. In this context, the intrinsic strain that develops in the film as part of the film deposition process is treated as a non-mechanical strain analogous to the thermal strains which typically appear in classical lamination theory. Thus,

$$\sigma_{x_s} = \frac{E_s}{1-\nu_s^2}(\varepsilon_x + \nu_s \varepsilon_y)$$

$$\sigma_{y_s} = \frac{E_s}{1-\nu_s^2}(\varepsilon_y + \nu_s \varepsilon_x)$$

$$\sigma_{x_f} = \frac{E_f}{1-\nu_f^2}(\varepsilon_x + \nu_f \varepsilon_y) - \frac{E_f e^i}{1-\nu_f}$$

$$\sigma_{y_f} = \frac{E_f}{1-\nu_f^2}(\varepsilon_y + \nu_f \varepsilon_x) - \frac{E_f e^i}{1-\nu_f} \tag{1}$$

where σ denotes stress, ε is strain, E is modulus, ν is Poisson's ratio and e^i is the intrinsic film strain. Subscripts s and f refer to the substrate and film respectively, while x and y refer to the coordinate system of Fig. 1. The strains ε_x and ε_y are the laminate strains which, according to classical lamination theory, are related to the strains and curvatures of the laminate middle plane by

$$\varepsilon_x = \varepsilon_x^\circ + z k_x$$

$$\varepsilon_y = \varepsilon_y^\circ + z k_y \tag{2}$$

where ε° and k denote the middle-plane strain and curvature, respectively.

Note from eqn (1) that for the limiting case of a rigid substrate (or of a "very thin" film), that the film stress approaches its fully constrained (or intrinsic) value

$$\sigma_f^i = -E_f e^i/(1-\nu_f). \tag{3}$$

If the substrate is not rigid, then the laminate middle-plane will stretch and bend and thus reduce the magnitude of the film stress below its intrinsic value. To determine the film stress for this case requires that we first determine the middle-plane strains and curvatures. The approach used for determining these quantities depends upon the assumed strain/displacement relations (linear or nonlinear) as discussed in the following two sections.

For the linear solution we employ the usual linear strain/displacement relations

$$\varepsilon_x = \frac{\partial u}{\partial x}$$

$$\varepsilon_y = \frac{\partial v}{\partial y}$$

$$2\varepsilon_{xy} = \frac{\partial u}{\partial y} + \frac{\partial v}{\partial x} \tag{4}$$

where u° and v° are the middle-plane displacements in the x and y directions, respectively. The nonlinear results are obtained by assuming von Kármán's (see, for example, Fung, 1965) strain/displacement relations

$$\varepsilon_x^\circ = \frac{\partial u^\circ}{\partial x} + \frac{1}{2}\left(\frac{\partial w^\circ}{\partial x}\right)^2$$

$$\varepsilon_y^\circ = \frac{\partial v^\circ}{\partial y} + \frac{1}{2}\left(\frac{\partial w^\circ}{\partial y}\right)^2$$

$$2\varepsilon_{xy}^\circ = \frac{\partial u^\circ}{\partial y} + \frac{\partial v^\circ}{\partial x} + \left(\frac{\partial w^\circ}{\partial x}\right)\left(\frac{\partial w^\circ}{\partial y}\right) \tag{5}$$

where w° is the displacement of the mid-plane in the z direction.

In both cases, the following relations between the middle-plane curvatures and displacements are assumed

$$k_x = -\frac{\partial^2 w^\circ}{\partial x^2}$$

$$k_y = -\frac{\partial^2 w^\circ}{\partial y^2}$$

$$k_{xy} = -\frac{\partial^2 w^\circ}{\partial x\,\partial y} \tag{6}$$

LINEAR SOLUTION

Since the laminate is assumed to be free of external constraints, the solution for the linear case may be obtained simply by requiring the net resultant forces and moments to vanish, i.e.

$$N_x = \int_{-h/2}^{h/2} \sigma_x \, dz = 0; \qquad N_y = \int_{-h/2}^{h/2} \sigma_y \, dz = 0$$

$$M_x = \int_{-h/2}^{h/2} \sigma_x z \, dz = 0; \quad M_y = \int_{-h/2}^{h/2} \sigma_y z \, dz = 0. \tag{7}$$

Substitution of eqns (1) and (2) into (7) and performing the indicated integrations yields a set of four equations that may be solved for the middle-plane strains and curvatures. The result is

$$\varepsilon^\circ = \varepsilon_x^\circ = \varepsilon_y^\circ = [A_5 + \tfrac{1}{2}RA_4(A_6 + A_7)/(A_2 + A_3)]e^i \tag{8a}$$

$$k^* = k_x^* = k_y^* = -A_4 e^i/(A_2 + A_3) \tag{8b}$$

where $k^* = h_s k$ is a nondimensional curvature, $R = h_f/h_s$ and the A_j are nondimensional

constants that depend upon R and upon the material properties of the film and substrate as defined in the Appendix.

Assuming that the curvature has been determined experimentally, eqn (8b) may be employed to determine the intrinsic film strain. If desired, the middle-plane strain could then be obtained from (8a) and the film stress from (1). Since the film stress will not (in general) be uniform across the film thickness, it may be more appropriate to calculate either an average film stress

$$\sigma_f^{avg} = \frac{1}{h_f}\int_{h/2-h_f}^{h/2} \sigma_{x_f}\,dz = \frac{E_f}{1-\nu_f}(\varepsilon^\circ + \tfrac{1}{2}k^* - e^i) \tag{9}$$

or the fully constrained film stress by eqn (3).

APPROXIMATE NONLINEAR SOLUTION

As a general rule of thumb, the linear results presented above may be considered valid whenever the maximum out-of-plane displacement is small (say, by at least an order of magnitude) with respect to the laminate thickness h. In order to extend the validity of our results to include those cases where the maximum out-of-plane displacement is of the same order of magnitude as h, it is necessary to consider the nonlinear strain/displacement relations of von Kármán [eqns (5)].

Due to the complexity of the nonlinear problem, a closed form solution relating the middle-plane strains and curvatures to the intrinsic film strain should not be expected. For this reason we decided to obtain an approximate solution by assuming kinematically admissible expressions for the middle-plane displacements in terms of several generalized coordinates whose values are determined by requiring a minimal value for the total potential energy of the laminate. Since the laminated beam is assumed free of external loadings, the total potential energy will be equal to the total strain energy which may be expressed as

$$U = \frac{1}{2}\int_{-a}^{a}\int_{-b}^{b}\left\{\int_{-h/2}^{h/2-h_f}(\sigma_{x_s}\varepsilon_x + \sigma_{y_s}\varepsilon_y)\,dz + \int_{h/2-h_f}^{h/2}(\sigma_{x_f}(\varepsilon_x - e^i) + \sigma_{y_f}(\varepsilon_y - e^i))\,dz\right\}dy\,dx. \tag{10}$$

The kinematically admissible middle-plane displacements are assumed to be as follows:

$$w^\circ = \tfrac{1}{2}(b_1x^2 + b_2y^2) \tag{11a}$$

$$u^\circ = c_1x - \tfrac{1}{6}b_1^2x^3 - \tfrac{1}{4}b_1b_2xy^2 \tag{11b}$$

$$v^\circ = c_2y - \tfrac{1}{6}b_2^2y^3 - \tfrac{1}{4}b_1b_2yx^2. \tag{11c}$$

These assumed forms were motivated by the work of Hyer (1981b) which analyzed the out-of-plane deflections of unsymmetric cross-ply composite laminates caused by the thermal strains which develop as that laminate cools from its elevated cure temperature. The primary assumption employed in arriving at eqns (11) is that the middle-plane curvatures of the laminate are spatially uniform. This conclusion was arrived at empirically by Hyer (1981b) for composite laminates and is also consistent with experimental observations for film/substrate laminates. The first term in eqns (11b) and (11c) represents the usual linear dependence of the in-plane displacements on the in-plane spatial coordinates that one would expect from linear theory. The second term in these equations represents the effects of the out-of-plane warping upon the in-plane displacements, while the last term is included to guarantee that the middle-plane shear strain vanishes. Since the laminate presently under consideration (Fig. 1) is a special type of asymmetric composite laminate (i.e. with isotropic rather than orthotropic layers) and since, from a mechanics point of view, the intrinsic film strain is analogous to a thermal strain, it would seem appropriate to consider eqns (11) as approximate expressions for the middle-plane deflections of our film/substrate laminate. The

importance of the assumed support conditions should be emphasized at this point since eqns (11) are clearly not kinematically admissible for the case of a clamped boundary.

The approximate nonlinear solution may now be obtained by substituting eqns (11) into eqns (5) and (6) with this result being substituted into eqns (1) and (2) and finally into eqn (10). Performing the indicated integrations then yields an explicit expression for the strain energy in terms of the generalized coordinates. Requiring the first variation of the strain energy with respect to the generalized coordinates to vanish yields a set of four nonlinear algebraic equations that may be solved for the generalized coordinates (Fox, 1954). These equations are very complicated and have been omitted here for brevity. It turns out that two of these equations are linear in c_1 and c_2 and may thus be readily solved in terms of b_1 and b_2 (or k_x^* and k_y^*). The result is

$$c_1 = \tfrac{1}{12}(b/h_s)^2 k_x^* k_y^* - \tfrac{1}{2}RA_6 k_x^* - \tfrac{1}{2}RA_7 k_y^* + A_5 e^i$$
$$c_2 = \tfrac{1}{12}(a/h_s)^2 k_x^* k_y^* - \tfrac{1}{2}RA_7 k_x^* - \tfrac{1}{2}RA_6 k_y^* + A_5 e^i \tag{12}$$

where the nondimensional constants A_5, A_6 and A_7 are given in the Appendix. Substitution of (12) into the remaining two equations yields two nonlinear algebraic equations for k_x^* and k_y^*, namely

$$A_1(a/h_s)^4(1+(b/a)^4)k_x^* k_y^{*2} + A_2 k_x^* + A_3 k_y^* + A_4 e^i = 0$$
$$A_1(a/h_s)^4(1+(b/a)^4)k_x^{*2} k_y^* + A_2 k_y^* + A_3 k_x^* + A_4 e^i = 0 \tag{13}$$

where A_1–A_4 are again given in the Appendix. For clarity, all dependence upon the in-plane dimensions a and b and the intrinsic strain e^i have been shown explicitly in eqns (12) and (13). The constants A_j depend only on the thickness ratio and the material properties.

It is interesting to note that as the in-plane dimensions approach zero, the solutions to eqn (13) approach the linear solution given in eqn (8b). Also, if this solution is substituted into (12), then c_1 and c_2 approach the linear solutions for ε_x° and ε_y°. This result is actually not very surprising since, as the in-plane dimensions become smaller, the ratio of the maximum out-of-plane deflection to the plate thickness will also decrease eventually reaching a value for which the linear solution is an acceptable approximation.

Inspection of eqns (13) also shows that an identical set of equations is recovered if we replace k_x^* by k_y^* and k_y^* by k_x^*. Thus, one solution of these equations will always have the property that $k_x^* = k_y^*$. Since these equations are nonlinear, other solutions are of course possible and do indeed occur in some situations. In fact, it can be readily shown that the following two solutions also satisfy eqns (13)

$$k_x^* = -\frac{A_4 e^i}{2A_2} \pm D$$
$$k_y^* = -\frac{A_4 e^i}{2A_2} \mp D \tag{14}$$

where

$$D = \frac{1}{2}\sqrt{\frac{A_1(A_4 e^i)^2(1+(b/a)^4) - 4(h_s/a)^4 A_2^2(A_2 - A_3)}{A_1 A_2^2(1+(b/a)^4)}}. \tag{15}$$

Note, however, that these two solutions are not always real. If the film is thin enough so that the terms containing R^2 in the expressions for A_2 and A_3 (see Appendix) can be neglected, then it can be shown that the quantity $A_2 - A_3$ is always positive. Since A_1 is also always positive, the two solutions given in eqn (14) will be either real or complex depending upon the relative magnitude of the two terms in the numerator of (15). Thus, for those

situations where D is imaginary there will be only one physically meaningful solution to eqns (13), i.e. the equal curvature shape where $k_x^* = k_y^*$. If D is real, however, eqn (13) will have three solutions. The case where the two terms in the numerator of (15) have equal magnitudes ($D = 0$) thus represents a bifurcation point in the nonlinear results. From this condition, the following expression for the intrinsic strain at this bifurcation point can be obtained

$$|e^i| = \frac{2A_2(h_s/a)^2}{A_4}\sqrt{\frac{A_2 - A_3}{A_1(1+(b/a)^4)}}. \tag{16}$$

Combining eqn (16) with (14) (with $D = 0$) provides a similar criteria for locating the bifurcation point in terms of the nondimensional curvature

$$|k^*| = (h_s/a)^2\sqrt{\frac{A_2 - A_3}{A_1(1+(b/a)^4)}}. \tag{17}$$

For applications involving the bending-plate experiment, eqn (17) has greater practical value than does (16) since it is the curvature that is measured directly in this experiment. To avoid the confusion associated with the prediction of multiple solutions for an experiment, it is desirable to design the experiment so that the measured curvatures will be always less than the value given by (17). Satisfying these criteria will not, however, guarantee that nonlinear geometric effects will be negligible as will be shown later.

Whenever multiple solutions are possible it is necessary to determine which, if any, of these are stable. This may be accomplished by investigating the second variation of the strain energy with respect to the generalized coordinates (Fox, 1954). Without going into details, it has been found that whenever the bifurcation point has not been reached, the single solution $k_x^* = k_y^*$ is always stable. After the bifurcation point has been exceeded, however, the two solutions represented by eqns (14) are always stable, whereas the equal curvature solution $k_x^* = k_y^*$ is always unstable.

RESULTS

Results will now be presented comparing the solutions obtained from the linear and nonlinear theories developed in the previous two sections for a variety of situations. Unless stated otherwise, all results are based on the following material properties and geometrical parameters that are typical for a metallic film on a glass substrate:

$$\begin{aligned} E_s &= 50\,\text{GPa} \\ E_f/E_s &= 4 \\ \nu_f = \nu_s &= 0.25 \\ e^i &= -0.003 \\ b/a &= 0.25 \\ a/h_s &= 200 \\ h_f/h_s &= 0.001. \end{aligned} \tag{18}$$

It is interesting to note that the assumed intrinsic strain produces a tensile (fully constrained) film stress of 800 MPa. This stress is very large, but is typical of those reported in the literature. For example, Klokholm and Berry (1968) calculated intrinsic film stresses for a number of metals and found these stresses to range between 100 and 1500 MPa.

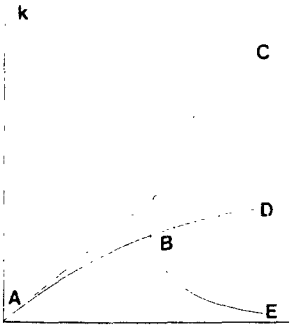

Fig. 2. Typical results of the linear and nonlinear models.

All results will show the predicted non-dimensional curvature versus some non-dimensional material or geometrical parameter of interest as depicted schematically in Fig. 2. Linear solutions will always be shown by a dashed line, while stable nonlinear solutions will be given by solid lines. Unstable solutions of the nonlinear equations will be represented by a dashed line with inserted dots. To conserve space, both curvatures k_x^* and k_y^* are plotted on the same axes with a particular point on a curve representing either k_x^* or k_y^*. For example, the dashed curve giving the linear solution always represents an equal curvature shape with $k_x^* = k_y^*$. The curve AB in Fig. 2 represents a situation where only one solution of the nonlinear equations is found. This solution is always found to be stable with $k_x^* = k_y^*$. Point B represents the bifurcation point after which the nonlinear theory will always provide three solutions. One of these solutions, represented by curve BD, will again have the property that $k_x^* = k_y^*$. This curve will always appear as an extension of curve AB and will always be unstable. The other two solutions are those predicted by eqns (14) and are given by curves BC and BE. Again, these two solutions are always stable. Letting subscripts BC and BE refer to the results depicted by curves BC and BE respectively, these two solutions are

$$k_x^* = k_{BC}^*; \quad k_y^* = k_{BE}^*$$

and

$$k_x^* = k_{BE}^*; \quad k_y^* = k_{BC}^*. \tag{19}$$

A general feature of these two solutions is that they will produce shapes that rapidly approach that of a right circular cylinder ($|k_x^*| \gg |k_y^*|$ or $|k_y^*| \gg |k_x^*|$). This tendency can be seen directly from eqns (14) and (15). For example, suppose that Fig. 2 represents the results for the non-dimensional curvature as a function of intrinsic strain (actual results for this case are given in Fig. 6) with all other parameters held constant. For this case, the first term in the numerator of eqn (15) will increase with increasing e^i while the second term (along with the denominator) will remain constant. For small values of e^i, D will be imaginary so that only one real solution exists (i.e. the solution $k_x^* = k_y^*$ given by curve AB in Fig. 2). As e^i increases, it will eventually reach the critical value given by eqn (16) which corresponds to the bifurcation point B in Fig. 2. When e^i exceeds this critical value, the two solutions represented by eqn (14) (curves BC and BE in Fig. 2) will become real. As e^i continues to increase, it will eventually become large enough so that the second term in the numerator of (15) will become negligible in comparison with the first. When this happens, the solutions of eqns (14) will approach the following

$$k_x^* \cong 0, \; -A_4 e^i / A_2$$
$$k_y^* \cong -A_4 e_i / A_2, \; 0. \tag{20}$$

It should be mentioned here that two distinct cylindrical shapes have been observed experimentally for unsymmetrical cross-ply composite laminates by Hyer (1981a). These laminates may be easily "flipped" back and forth between these two stable cylindrical shapes by applying a small amount of pressure to the center of the laminate.

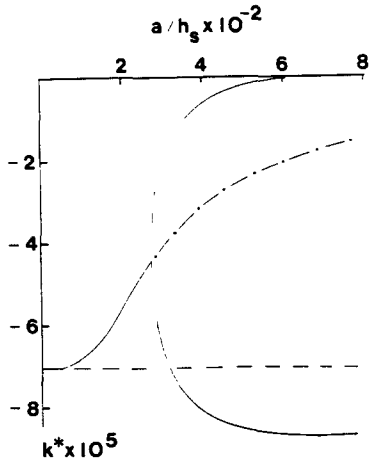

Fig. 3. The effect of the specimen length to substrate thickness ratio upon the non-dimensional curvature of a film/substrate laminate.

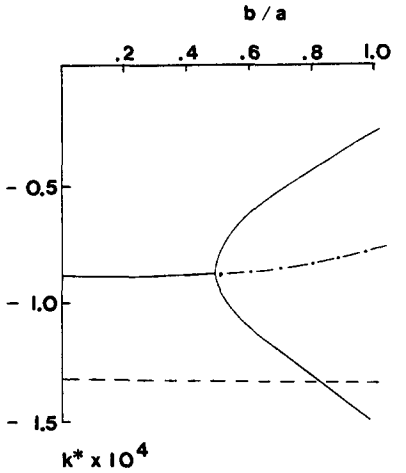

Fig. 4. The effect of width to length ratio upon the non-dimensional curvature.

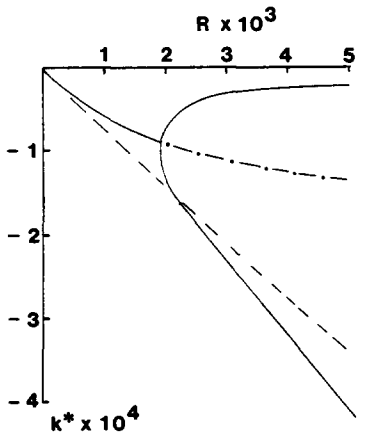

Fig. 5. Non-dimensional curvature as a function of film to substrate thickness ratio.

Figures 3–7 show specific results for the non-dimensional curvature k^* as a function of the non-dimensional parameters a/h_s, b/a, h_f/h_s, e^i and E_f/E_s. In some of these cases (in particular, Figs 5–7) there is an apparent tendency for the linear solution to approach the larger of the two nonlinear solutions beyond the bifurcation point. Comparing eqns (8b)

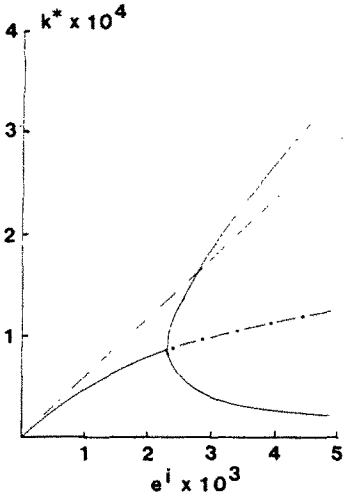

Fig. 6. The effect of the intrinsic film strain upon the non-dimensional curvature.

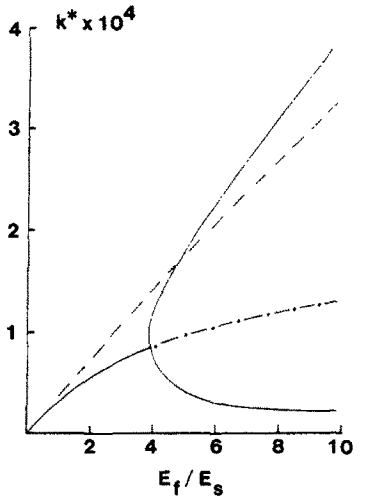

Fig. 7. Non-dimensional curvature as a function of the film/substrate modulus ratio.

and (20) it is seen that the ratio of the linear solution (k_l^*) to the larger nonlinear solution (k_{nl}^*) beyond the bifurcation point approaches the value

$$k_l^*/k_{nl}^* = A_2/(A_2+A_3). \tag{21}$$

Due to the complexity of the non-dimensional parameters A_2 and A_3, it is difficult to say much in general about eqn (21) except to note that for the special case where the film is thin enough so that terms containing R^2 may be neglected and if $\nu_f = \nu_s = \nu$ (as considered here), then (21) reduces to

$$k_l^*/k_{nl}^* = 1/(1+\nu). \tag{22}$$

Thus, if $\nu = 0.25$ then the linear solution will approach a value that is 80% of the larger nonlinear solution beyond the bifurcation point.

Figures 3 and 4 show the pronounced effect of the in-plane dimensions of a specimen upon the curvature. These results are important from a practical point of view since all results for intrinsic stresses in thin films reported in the literature are calculated based on a linear theory which is independent of the in-plane dimensions of the specimen. Figure 3 is based upon the parameters given in eqn (18) except that the ratio a/h_s varies between 0 and 800. The bifurcation point for the case considered in Fig. 3 occurs when a/h_s reaches

approximately 280; however, this value may decrease significantly if E_f/E_s, h_f/h_s, or the magnitude of the intrinsic strain e^i are increased from the values given in (18). The difference between the predictions based upon the linear and nonlinear theories at the bifurcation point in Fig. 3 is roughly 45%.

Figure 4 is similar to Fig. 3 except that the ratio b/a varies between 0 and 1 with a/h_s held constant at a value of 200. Thus, this figure illustrates the effects of changing the in-plane geometry of the specimen from that of a beam to a rectangular plate and finally to a square plate. In order to illustrate the fact that such changes may cause a bifurcation point in the nonlinear results, the film to substrate thickness ratio has been increased from 0.001 in Fig. 3 to 0.0019 in Fig. 4. The critical point for Fig. 4 occurs for a rectangular plate with $b/a \simeq 0.5$. Again, any increase in E_f/E_s, h_f/h_s or e^i will cause this critical ratio to decrease. In fact, there are many instances where the nonlinear solution will be beyond the bifurcation point for all values of b/a.

Figure 5 illustrates the effects of increasing the film to substrate thickness ratio while holding all other parameters constant at the values specified in (18). These results are also of practical significance since experimental results are commonly presented in the literature as a function of film thickness. The predictions of the linear and nonlinear theories are practically identical up to a thickness ratio $h_f/h_s \simeq 7 \times 10^{-4}$. Following this, the two solutions diverge rapidly with a roughly 45% discrepancy being observed at the bifurcation point where $h_f/h_s \simeq 2 \times 10^{-3}$. These specific observations in terms of thickness ratios are valid only for the case shown in Fig. 5 and will be significantly affected by any change in the modulus ratio, intrinsic strain, or substrate dimensions. Also, it is misleading to compare the magnitudes of the curvatures predicted after the critical point is reached since the two theories predict fundamentally different shapes beyond this point (i.e. the linear theory predicts an equal curvature shape while the nonlinear theory predicts two approximately cylindrical shapes). From a practical point of view, it is extremely important to guarantee that the bifurcation point has not been exceeded during a bending-plate experiment. The reason for this is that during a typical experiment one would usually employ a beam-like specimen and measure the curvature along the specimen's length direction (i.e. k_x). If the critical point has been exceeded, however, there are two possible values for this curvature, and it is impossible to know *a priori* which of these is being measured.

Figure 6 shows the effect of the intrinsic film strain upon the curvature of a film/substrate laminate. In view of eqn (3), this figure may also be interpreted in terms of the fully constrained (or intrinsic) film stress σ_f^i. For small values of the intrinsic strain (or stress), the linear and nonlinear predictions are practically identical; however, as the intrinsic strain increases, the discrepancy between these predictions increases reaching around 45% at the bifurcation point where $e^i = 0.0023$ ($\sigma_f^i = -613$ MPa).

Figure 7 illustrates the effects of the film/substrate modulus ratio E_f/E_s. All other parameters are as given in eqn (18) except that $e^i = +0.003$. This figure has practical significance since many early investigations calculated the intrinsic film stress from a simplified formula that neglected any difference between the film and substrate moduli. This will obviously produce significant errors since for the typical case of a metallic film on a glass substrate, the modulus ratio will usually be in the range from 3 to 5. In Fig. 7, this range contains the bifurcation point ($E_f/E_s = 3.8$).

This section will be concluded by making specific comparisons between the intrinsic film stress predicted by the linear and nonlinear models from experimental data that have appeared in the literature. Unfortunately, few comparisons of this type are possible since most published results fail to report the in-plane dimensions of the specimens employed. In what follows, experimentally determined curvatures are used to obtain the intrinsic film strain by eqn (8b) and (13) for the linear and nonlinear cases, respectively. Equation (3) is then employed to predict the intrinsic film stress in each case.

Before proceeding, it should be mentioned that in each case considered, the substrate was clamped at one end and the curvature determined by a displacement measured at the free end. As noted previously, the nonlinear model developed here is not strictly valid for this cantilevered support condition; however, in all cases except one the reported curvature is always less than the critical value at the bifurcation point as predicted by eqn (17).

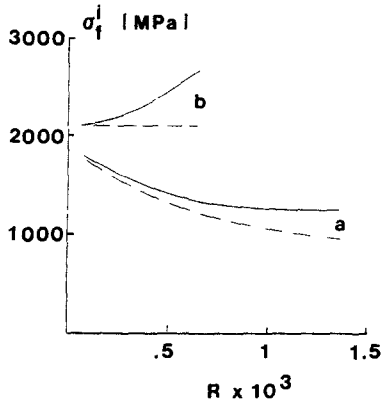

Fig. 8. Predictions of the intrinsic film stress by the linear (– – –) and nonlinear (— —) models based upon the experimental data of Abermann and Martinz (1984).

Recall that the nonlinear theory always predicts an equal curvature shape ($k_x^* = k_y^* = k^*$) wherever the bifurcation point has not been reached and that the linear theory also predicts this same general shape with, of course, a different value for k^*. Thus, the linear theory also fails to satisfy boundary conditions at a cantilevered support since one of the two principal curvatures must be zero at this support. It would only be appropriate to employ this theory to the cantilevered case if the curvature were calculated based upon the *relative* displacement between two or more points that are located well away from the clamped support. In practice, however, the curvature is usually calculated from a single deflection measured at the free end of the specimen. In our opinion, the possibility that this measured tip deflection might be affected by a clamped boundary has not been adequately addressed in the literature. In any event, the purpose for making the following comparisons is not to argue that either of the models developed here is strictly valid for the cantilevered beam case, but rather to illustrate the errors that are possible whenever nonlinear effects are ignored by using actual experimental data that have appeared in the literature.

Figure 8 gives comparisons between the intrinsic film stress predicted by the linear and nonlinear models as a function of the film to substrate thickness ratio R. These results are based upon the experimental data of Aberman and Martinz (1984) for a chromium film deposited at a constant rate onto a glass, cantilevered substrate. The curves labeled a and b in this figure correspond to the curves with the same labels in Fig. 2 of Aberman and Martinz (1984). Curve a was obtained with the substrate at room temperature, while for curve b the substrate was at 160°C. In both cases, the dashed line gives predictions based upon the geometrically linear model [eqn (8b)], while the solid line gives the nonlinear predictions [eqn (13)]. It turns out that the critical value for the nondimensional curvature k^* at the bifurcation point [as predicted by eqn (17)] is practically independent of the film thickness for the relatively small film to substrate thickness ratios encountered in these tests. This critical value is about 1.6×10^{-4}, whereas the maximum experimentally determined values for k^* are roughly 1×10^{-4} for both curves a and b. These maximum values occur at the end of the test when the film thickness reaches its maximum value, which is also the maximum value for R since h_s is constant. Thus, the theoretical bifurcation point has not been exceeded in either of these tests.

The discrepancy between the linear and nonlinear predictions in Fig. 8 (expressed as a percentage of the linear result) is around 25% for both cases. Also, the ratio of the maximum displacement to substrate thickness is roughly 4 for both tests. It is interesting to note that the linear model predicts an instrinsic film stress that is practically independent of film thickness for case b, whereas the nonlinear model predicts a film stress that increases with increasing film thickness. Also note that in both cases the nonlinear model predicts higher values for the intrinsic film stress than does the linear model. This observation will be discussed in greater detail later.

Figure 9 is similar to Fig. 8 except that the results are based on data from Horikoshi and Tamura (1963) for an antimony film deposited onto a cantilevered copper substrate.

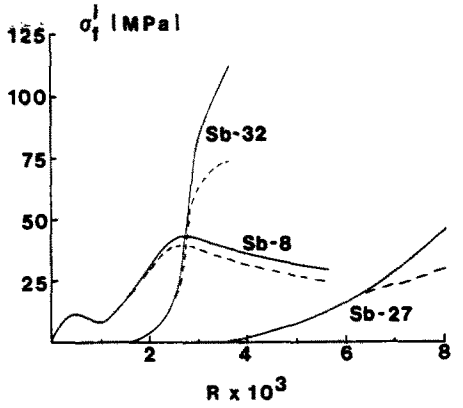

Fig. 9. Predictions of the intrinsic film stress by the linear (– – –) and nonlinear (— —) models based upon the experimental data of Horikoshi and Tamura (1963).

The labels in Fig. 9 are the specimen numbers as given in Fig. 6 of Horikoshi and Tamura (1963). All data were obtained with the substrate at room temperature with constant film deposition rates of 350, 1500 and 9500 Å min^{-1} for specimens Sb-8, Sb-32 and Sb-27, respectively. Specimens Sb-27 and Sb-32 displayed relatively small compressive film stresses initially; however, the results shown in Fig. 9 begin where the film stress became tensile.

As with the previous case, the critical value for k^* at the bifurcation point is practically independent of R for the range of film thicknesses considered here. This value is about 8.8×10^{-6} with a maximum error of roughly 3% for the range of R considered. Generally speaking, the measured curvature in this type of test is always found to increase with increasing film thickness so that the maximum k^* values occur at the maximum values for R in Fig. 9. For specimen Sb-8, this maximum k^* value is about 4.9×10^{-6}, well below the theoretical bifurcation point. For specimen Sb-27, the maximum k^* value is around 8.3×10^{-6}, which is very close to the theoretical critical value of 8.8×10^{-6}. The maximum values for k^* for the results shown for specimen Sb-32 is exactly 8.8×10^{-6}, which is the critical value according to eqn (17). The data reported by Horikoshi and Tamura (1963) actually extended beyond this point (out to $R \simeq 0.004$); however, calculations based on this data are not shown in Fig. 9 since they exceed the theoretical bifurcation point. The maximum discrepancies between the linear and nonlinear predictions (as a percentage of the linear value) are roughly 15, 45 and 55% for specimens Sb-8, Sb-27 and Sb-32, respectively, while the ratio of the maximum displacement to the substrate thickness is about 3.6, 6 and 6.3, respectively.

It is noted in Figs 8 and 9 that the value for the intrinsic stress predicted by the nonlinear model is always larger than that predicted by the linear results. It may be readily shown that this result is true in general provided that the film is relatively thin (where relatively thin means that R^2 may be considered very small in comparison with unity) and that the bifurcation point has not been exceeded. Assuming that the bifurcation point has not been reached, we may substitute $k_x^* = k_y^* = k^*$ into eqns (13) and combine this result with eqn (3) to yield the following expression for the intrinsic film stress as a function of the nondimensional curvature:

$$-\sigma_f^i = \frac{E_s}{2R(1-\nu_s^2)(1+RB_8/B_1)}\left[A_1\left(\frac{a}{h_s}\right)^4(1+(b/a)^4)k^{*3}+(A_2+A_3)k^*\right]. \quad (23)$$

It can be shown that the term containing k^* in eqn (23) is identical to the linear solution that would be obtained by combining eqn (8b) with eqn (3). Thus the term containing k^{*3} accounts for the nonlinear geometric effects upon the intrinsic film stress. It can also be shown that the two coefficients multiplying k^* and k^{*3} in eqn (23) will always have the same sign provided that $R^2 \ll 1$. Thus the magnitude of the intrinsic stress predicted by the nonlinear model will always exceed that of the linear model for this case. This means that

a prediction based upon the linear results will *not* provide a conservative estimate of the intrinsic film stress.

CONCLUSIONS

This paper presented a model capable of accounting for nonlinear geometric effects in the bending-plate experiment that is commonly employed to estimate the intrinsic stress in thin films. A linear model was also developed that is valid for any film thickness. Previous linear models that have been applied to this experiment have all assumed that the film is thin in comparison with the substrate.

Several results were presented based upon material properties and geometrical parameters that are typical of many bending-plate experiments. It is clear from these results that significant errors may result due to the neglect of nonlinear geometric effects. Comparisons between the predictions of the linear and nonlinear models were also made based upon actual experimental data. Of the cases considered, the maximum discrepancies between the two models ranged from 15 to 55%. Based upon these observations, it seems possible that nonlinear geometric effects may be (at least partially) responsible for some of the discrepancies that have appeared in the literature where different investigators have reported significantly different film stresses for the same material.

Probably the most practical conclusion to be drawn from this study is the need for properly designing a bending-plate experiment. Since the nonlinear model presented here is probably too cumbersome to employ in practice, it is important to be able to design an experiment so that nonlinear effects will be negligible over the entire range of parameters that are of interest. Precisely how this may be accomplished is the subject of a forthcoming paper. Also to be shown in this paper is the relation between the present linear model and those that have been employed in the past.

REFERENCES

Abermann, R. and Martinz, H. P. (1984). Internal stress and structure of evaporated chromium and MgF_2 films and their dependence on substrate temperature. *Thin Solid Films* **115**, 185–194.

Brenner, A. and Senderoff, S. (1949). Calculation of stress in electrodeposits from the curvature of a plated strip. *J. Res. Nat. Bur. Stand.* **42**, 105–123.

Chopra, K. L. (1969). *Thin Film Phenomena*, Chapter V. McGraw-Hill, New York.

Fox, C. (1954). *An Introduction to the Calculus of Variations*. Oxford University Press, London.

Fung, Y. C. (1965). *Foundations of Solid Mechanics*. Prentice-Hall, Englewood Cliffs, New Jersey.

Hoffman, R. W. (1966). In *Physics of Thin Films* (Edited by G. Hass and R. E. Thun), Vol. 3, p. 211. Academic Press, New York.

Horikoshi, H. and Tamura, N. (1963). Internal stress and electrical resistivity of evaporated antimony films. *Jap. J. Appl. Phys.* **2**, 328–336.

Hyer, M. W. (1981a). Some observations on the cured shape of thin unsymmetric laminates. *J. Comp. Mat.* **15**, 175–194.

Hyer, M. W. (1981b). Calculations of the room temperature shapes of unsymmetric laminates. *J. Comp. Mat.* **15**, 296–310.

Jones, R. M. (1975). *Mechanics of Composite Materials*. McGraw-Hill, New York.

Kinosita, K. (1972). Recent developments in the study of mechanical properties of thin films. *Thin Solid Films* **12**, 17–28.

Klokholm, E. and Berry, B. S. (1968). Intrinsic stress in evaporated metal films. *J. Electrchem. Soc.: Sol. St. Sci.* **118**, 823–826.

Stoney, G. G. (1909). The tension of metallic films deposited by electrolysis. *Proc. R. Soc. London [A]* **82**, 172–175.

APPENDIX

The non-dimensional constants A_1–A_7 that appear in eqns (5), (12) and (13) of the text are as follows:

$$A_1 = \tfrac{1}{15}(1+RQ)$$

$$A_2 = B_2 - R^2B_3/B_1$$

$$A_3 = B_4 + R^2B_5/B_1$$

$$A_4 = -2RQ(1+\nu_f)(1+RB_8/B_1)$$

$$A_5 = RQ(1+\nu_f)(1-\nu_s+RQ(1-\nu_f))/B_1$$

$$A_6 = [RQ^2(1-v_f^2)-(1-v_s^2)+Q(1-R)(1-v_s v_f)]\ B_1$$

$$A_7 = Q(1+R)(v_f-v_s)/B_1$$

where

$$R = h_f/h_s$$

$$Q = E_f(1-v_s^2)/E_s(1-v_f^2)$$

$$B_1 = (1+RQ)^2-(v_s+RQv_f)^2$$

$$B_2 = \tfrac{1}{3}(1+3R^2+RQ(3+R^2))$$

$$B_3 = (1+RQ)B_6-2(v_s+RQv_f)B_7$$

$$B_4 = \tfrac{1}{3}((1+3R^2)v_s+RQ(3+R^2)v_f)$$

$$B_5 = (v_s+RQv_f)B_6-2(1+RQ)B_7$$

$$B_6 = (1-Q)^2+(v_s-Qv_f)^2$$

$$B_7 = (1-Q)(v_s-Qv_f)$$

$$B_8 = (1-v_s+RQ(1-v_f))(1+v_s-Q(1+v_f)).$$